

Shallow Water Propagation

William L. Siegmann
Rensselaer Polytechnic Institute
110 Eighth Street
Jonsson-Rowland Science Center 1C08
Troy, New York 12180-3590
phone: (518) 276-6905 fax: (518) 276-2825 email: siegmw@rpi.edu

Adam M. Metzler
Rensselaer doctoral student

Kara G. McMahon
Rensselaer doctoral student

Award Numbers: N000140410016
N000140810972 (Ocean Acoustics Graduate Traineeship)
N000140910638 (Ocean Acoustics Graduate Traineeship)
http://www.math.rpi.edu/www/ocean_acoustics

LONG-TERM GOALS

Develop methods for deterministic and stochastic acoustic calculations in complex shallow water environments, specify their capabilities and accuracy, and apply them to understand experimental data and physical mechanisms of propagation.

OBJECTIVES

- (A) Treat propagation from narrowband and broadband sources over elastic and poro-elastic sediments, and incorporate realistic bathymetric, topographic, and geoacoustic variations.
- (B) Quantify acoustic interactions with physical features in the ocean volume and with geoacoustic features of the ocean sediment, and analyze and interpret experimental data.

APPROACH

- (A) Develop efficient and accurate parabolic equation (PE) techniques for propagation through heterogeneous sediments. Treat range dependence and sediment layering by single scattering and energy conservation methods. Benchmark results using data and special high-accuracy solutions.
- (B) Construct representations for ocean environmental and geoacoustic variability using data and parametric models. Determine acoustic fields with PE, normal mode, and approximation methods. Use experimental data and computational results to assess propagation mechanisms.

Report Documentation Page				Form Approved OMB No. 0704-0188	
Public reporting burden for the collection of information is estimated to average 1 hour per response, including the time for reviewing instructions, searching existing data sources, gathering and maintaining the data needed, and completing and reviewing the collection of information. Send comments regarding this burden estimate or any other aspect of this collection of information, including suggestions for reducing this burden, to Washington Headquarters Services, Directorate for Information Operations and Reports, 1215 Jefferson Davis Highway, Suite 1204, Arlington VA 22202-4302. Respondents should be aware that notwithstanding any other provision of law, no person shall be subject to a penalty for failing to comply with a collection of information if it does not display a currently valid OMB control number.					
1. REPORT DATE 2010		2. REPORT TYPE		3. DATES COVERED 00-00-2010 to 00-00-2010	
4. TITLE AND SUBTITLE Shallow Water Propagation				5a. CONTRACT NUMBER	
				5b. GRANT NUMBER	
				5c. PROGRAM ELEMENT NUMBER	
6. AUTHOR(S)				5d. PROJECT NUMBER	
				5e. TASK NUMBER	
				5f. WORK UNIT NUMBER	
7. PERFORMING ORGANIZATION NAME(S) AND ADDRESS(ES) Rensselaer Polytechnic Institute, 110 Eighth Street, Jonsson-Rowland Science Center 1C08, Troy, NY, 12180-3590				8. PERFORMING ORGANIZATION REPORT NUMBER	
9. SPONSORING/MONITORING AGENCY NAME(S) AND ADDRESS(ES)				10. SPONSOR/MONITOR'S ACRONYM(S)	
				11. SPONSOR/MONITOR'S REPORT NUMBER(S)	
12. DISTRIBUTION/AVAILABILITY STATEMENT Approved for public release; distribution unlimited					
13. SUPPLEMENTARY NOTES					
14. ABSTRACT					
15. SUBJECT TERMS					
16. SECURITY CLASSIFICATION OF:			17. LIMITATION OF ABSTRACT Same as Report (SAR)	18. NUMBER OF PAGES 10	19a. NAME OF RESPONSIBLE PERSON
a. REPORT unclassified	b. ABSTRACT unclassified	c. THIS PAGE unclassified			

- Principal collaborators are: Rensselaer graduate students and recent graduates; Dr. Michael Collins (NRL), for model development; and Profs. William Carey and Allan Pierce (BU), and Drs. James Lynch and Timothy Duda (WHOI), for theoretical interpretations and data analysis.

WORK COMPLETED

(A) Propagation model development

(1) *Accurate calculations for range-dependent elastic sediments*

- A single-scattering approximation combined with a coordinate rotation technique handles ocean seismo-acoustic problems with range-dependent bathymetry, variable thickness sediment layers, and topographic variations for beach, island, and coastal problems [1].
- Accuracy of the new PE method is confirmed by comparisons [2] with high fidelity data from propagation over an elastic slab with variable bottom slopes in a large NRL tank.
- Accuracy is also verified by comparing with benchmarks for problems with large changes in sound speeds and with waves on range-dependent elastic interfaces [3], and guidelines for selection of computational parameters are determined.

(2) *New capabilities for range-dependent elastic sediments*

- Generalization of the PE method permits treatment of range-dependent transversely isotropic elastic sediments [4] which occur in many coastal regions, and examples of anisotropic effects on propagation are provided.
- Reformulation of the propagation variables produces a new method [5] with the potential of treating range dependent bathymetry and elastic interfaces more efficiently, and at least as accurately, as the best currently available methods.

(3) *Accurate calculations for range-dependent poro-elastic sediments*

- The first propagation model able to handle weak range dependence in transversely isotropic poro-elastic sediments [6] shows the feasibility of PE approaches.
- Recent progress for range-dependent elastic sediments is extended to poro-elastic sediments [7], by employing the same propagation variables and computational techniques as in [3].
- A new method for poro-elastic media is constructed [8], based on the variable reformulation in [5], to treat range dependence efficiently and accurately, and initial benchmarking of the implementation is demonstrated.

(B) Propagation mechanism assessment

(1) *Nonlinear internal wave propagation effects*

- In the presence of nonlinear internal wave fronts, acoustic modes may propagate adiabatically and interact at small incident angles with the fronts to form horizontal Lloyd mirror interference patterns [9], which are particularly interesting when the fronts are curved.

- To improve specification of acoustic effects from nonlinear internal waves, feature parameters are estimated from satellite SAR images [10], with accuracy tested by comparisons with ground truth mooring data.
- Fully three-dimensional propagation calculations show that horizontal mode coupling may arise from two or more interacting nonlinear internal waves [11], depending on their amplitudes, orientations, and coherence lengths.
- A scattering formalism, based on a limit of discrete scattering events and a modal transport theory, provides an alternative description of intensity variations in a nonlinear internal wave duct [12], and is compared with the standard refractive treatment.

(2) *Modal attenuation coefficient variability*

- Nonlinear frequency dependence of sediment attenuation has substantial effects that can be physically interpreted by using a parametric description for a Pekeris waveguide and examining the frequency behavior of modal attenuation coefficients [13].
- Attenuation coefficients obtained from a normal mode approach agree well with earlier estimates found from Gulf of Mexico data [14], after identifying and using an appropriate subset of measured sound speed profiles.
- Nonlinear frequency dependence in sediment attenuation and thermocline-type water sound speed profiles can produce significant sensitivity in the frequency dependence of modal attenuation coefficients [15].
- New asymptotic approximations for modes are used to show that the location and strength of sound speed gradients in the water column have significantly different effects on the parametric dependence of modal attenuation coefficients [16].

(3) *Transmission loss dependence on intrinsic sediment attenuation*

- The connection between the frequency dependence of modal attenuation coefficients and an overall linear attenuation of averaged reduced transmission loss is quantified [17] by showing the primary dependence on water sound speed profile features.
- Nonlinear frequency dependence of intrinsic sediment attenuation behavior is necessary [18] for good agreement between New Jersey AGS data and broadband intensity calculated with variations due to geoacoustic uncertainties.
- Efficient methods are developed for recent experimental sites, to find relationships between the frequency power law of intrinsic attenuation, modal attenuation coefficients, and averaged transmission loss [19], in order to assess the robustness of earlier power law estimates.
- Relatively simple formulas for averaged transmission loss in range-independent waveguides are derived from mode theory, and they reduce to results of Rogers and others for high frequencies and isospeed or constant gradient water sound speed profiles [20].

(4) *Consequences of the cardhouse theory of mud*

- The electric charge on bubbles is an important feature of this model, and under simplified uniform conditions the charged bubbles are not spherical [21], which is in accord with experimental observations.

- In this theory mud platelets are hypothesized to behave like electrical quadrupoles, and an estimate of shear wave speed is obtained by computing the oscillation frequency of a hinged joint formed by platelets which interact end to side [22].

RESULTS (from two selected investigations)

- (A) Acoustic data analysis and other applications need capabilities for efficient and accurate propagation calculations in shallow water waveguides with range-dependent elastic sediments and interfaces. Sediment elasticity is important because energy transfer between compressional and shear modes may substantially modify acoustic intensity and phase. In addition, handling elasticity effectively is vital for producing extensions to poro-elastic, anisotropic, and other complex sediments. A key physical and computational issue is that energy spectra for elastic sediments extend over more wave numbers than for fluid sediment models. Our current PE method [1] developed from a series of advances, including formulation with non-standard dependent variables, employing coordinate rotations at range locations of bathymetry slope changes, using single- scattering corrections at stair-step approximations of changes in sediment interfaces and volume parameters, and incorporating a procedure to handle relatively large changes at stair steps. Benchmarking provides essential validation throughout the development, and one paper [2] shows applications to high quality data obtained from an NRL experimental series using elastic slabs. Additional calculations [3] show excellent agreement with benchmarks for problems with relatively large changes in sound speeds and with range-dependent interface waves. An important extension [4] is to range-dependent transversely isotropic (TI) elastic sediments which occur in coastal and shallow regions. **Figure 1** illustrates the accuracy and capability of our method for treating such sediments. Fig. 1(a) shows an accurate benchmark for reduced transmission loss in a range-dependent TI waveguide problem, and the corresponding picture (omitted) from the method is nearly identical. For example, Fig. 1(b) shows strong agreement between the benchmark and implementation calculations for reduced transmission loss on tracks 100 m below the upper interface. Next, two range-independent waveguides are examined, with an isotropic elastic layer over an elastic bottom that is either TI or “effective” isotropic (EI). The latter has isotropic sound speed values which best model TI layers. Figs. 1(c) and 1(d) are horizontal wave number spectra and transmission loss for a source near, and a receiver well above, the interface. Depending as usual on the accuracy level sought, the EI model acceptably represents the results from the TI sediment in this case. Figs. 1(e) and 1(f) are corresponding results for both source and receiver near the interface. The EI sediment does not acceptably model all features of the TI sediment, and consequently sediment anisotropy may need to be included rather than neglected or “averaged out”. We conclude from these and other results that our new propagation method provides essential capabilities for efficient and accurate calculations in waveguides with range variations in bathymetry, topography, and elastic sediment structure, anisotropy, and layering.
- (B) Nonlinear internal waves (NIWs), which are common in shallow water, cause significant variations in acoustic field amplitude and phase. Experiments from SWARM through SW06 show the strength and variety of such variations, and valuable modeling has been accomplished. Issues still remain, for example concerning assimilation of different types of NIW observations into environmental acoustics models, in order to take advantage of all available data and to improve NIW parameter estimates [10]. Another example is specifying when acoustic modes propagate through NIWs with and without cross-range mode coupling [11]. Our interest is also

in the interference patterns that develop as acoustic modes propagate coherently near a NIW front. This mechanism has been identified by our WHOI colleagues as a horizontal Lloyd mirror (HLM), because of the direct analogy with the traditional Lloyd mirror pattern near the sea surface. The clearest example occurs when a single mode propagates adiabatically, to produce a HLM pattern with little or no acoustic penetration across the front and with “refraction” that is well modeled by “reflection” below critical angle. Previous treatments for essentially straight fronts show an expected dependence on source-receiver geometry. Of particular interest are trains of NIWs and those for which curvature is not negligible [9], as is typical in the ocean. With curvature the most direct solution approach uses Huygen’s Principle. Examples are shown in **Figure 2**, which displays reduced transmission loss contours for a sound-speed jump approximation of a circular NIW front. In Fig. 2(a) a front with large radius of curvature R produces a HLM pattern much like that from a straight front, with the dashed line and the front bounding a region of strong beams. With R smaller as in Fig. 2(b), the region of strong pattern decreases along with the beam spacing. For $R = 70$ km in Fig. 2(c), the changes accelerate so that the distant region with some cross-front transmission becomes visible. When R decreases to 50 km in Fig. 2(d), transmission occurs across the front almost everywhere since reflection angles are above critical, and the narrow HLM beams have weaker contrasts. We conclude from these and other calculations that horizontal Lloyd mirror interference patterns have significant variations not only with source-receiver geometry, but also with front shape and structure parameters and the number of NIWs in the train. An open question is whether these patterns and variations appear in experimental observations.

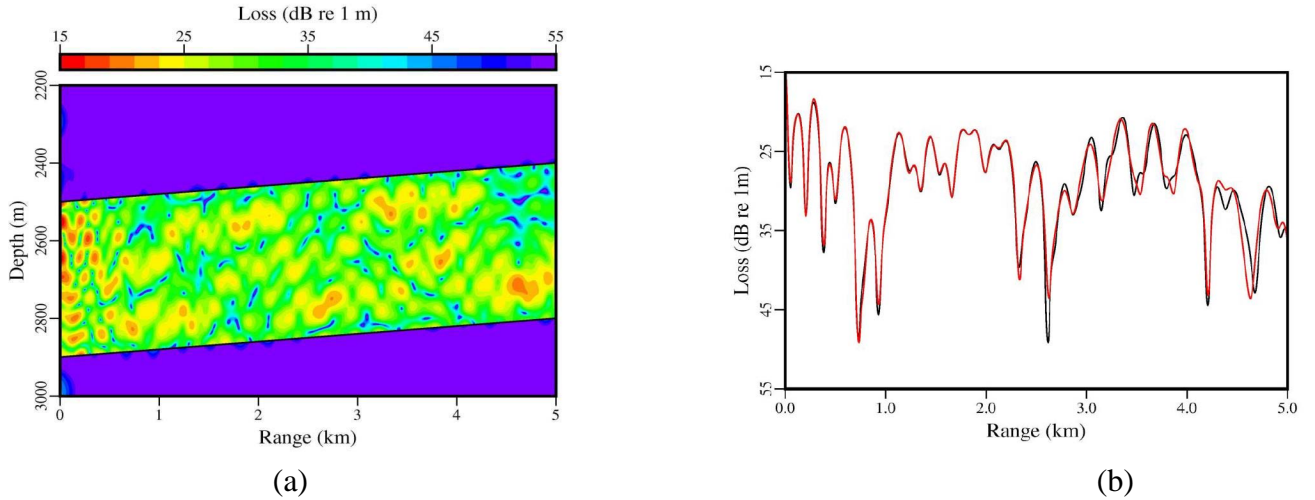
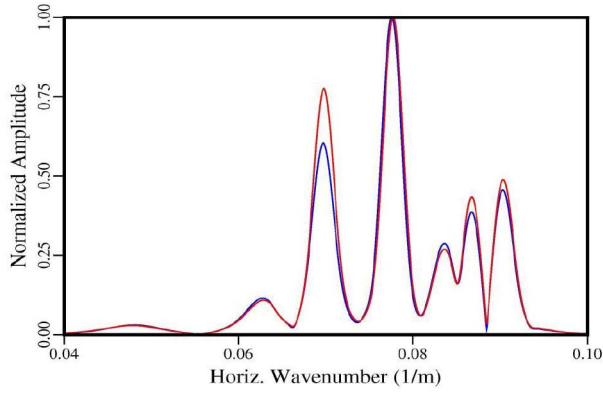
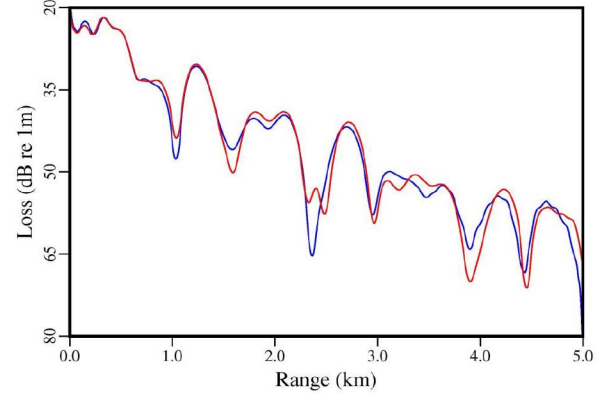


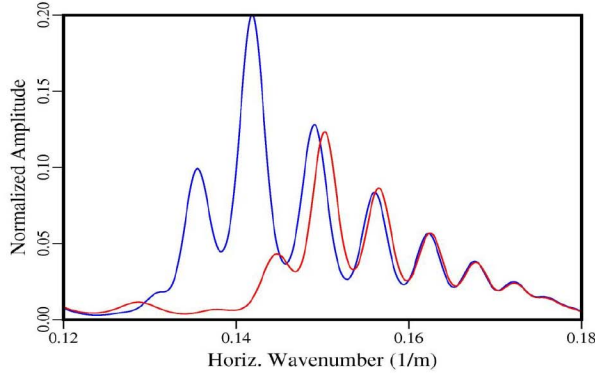
Figure 1. Accurate modeling of propagation in transversely isotropic (TI) elastic sediments is obtained from the single-scattering parabolic equation. *Fig. (a):* Color contours of reduced transmission loss between 15 and 55 dB (re: 1 m) over 5 km range for a benchmark environment, consisting of a TI elastic waveguide of 400 m thickness, $\rho = 1.5 \text{ gm/cm}^3$, and an upward slope 1.15° , which is sandwiched between two thick, high-density, isotropic elastic layers. The waveguide has anisotropic sound speed differences of $\delta c_p = 150 \text{ m/s}$ and $\delta c_s = 25 \text{ m/s}$, with a 10 Hz source 100 m below the upper interface. Contours for the benchmark and the range-dependent PE calculation (not shown) are almost identical. *Fig. (b):* Corresponding reduced (10logr removed) transmission loss curves on a track 100 m below the upper interface. The black curve is the benchmark solution, and the red curve is calculated by the range-dependent single scattering method. The agreement is excellent and shows an oscillatory pattern with about 250 m wavelength beyond 2 km.



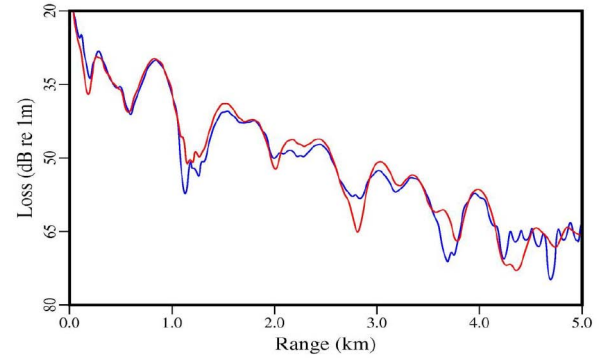
(c)



(d)



(e)



(f)

Figure 1. Fig. (c)-(f): Two range-independent elastic waveguides are compared, both having an isotropic upper layer of thickness 300 m, $c_p = 1700$ m/s, and $c_s = 850$ m/s, with a 25 Hz source located 5 m above the bottom interface. One waveguide (red curves) has a TI elastic bottom layer with $\delta c_p = 150$ m/s and $\delta c_s = 100$ m/s. The other (blue curves) has an “effective” isotropic (EI) elastic bottom with both compressional and shear wave speeds at their maxima in the TI layer, since such values give the best overall correspondence with TI cases. Fig. (c) compares horizontal wave number spectra between 0.04 and 0.10 /m, normalized with maximum-peak amplitude one, at 25 m depth. The next three largest TI c_p -wave peaks are underestimated by the EI peaks. Fig. (d) has corresponding transmission loss curves between 20 and 80 dB (re: 1 m) over 5 km range at 25 m depth. The agreement is acceptable before 2 km and deteriorates beyond. Fig. (e) compares spectra between 0.12 and 0.18 /m at 299 m depth, just above the interface. The TI curve shows an interface wave peak which is missing in the EI curve. Fig. (f) has corresponding transmission loss curves at 299 m, with acceptable agreement before 1 km and usually worse beyond. The single scattering TI propagation model has benchmark-comparable accuracy and demonstrates that anisotropic effects cannot generally be neglected for high fidelity propagation calculations.

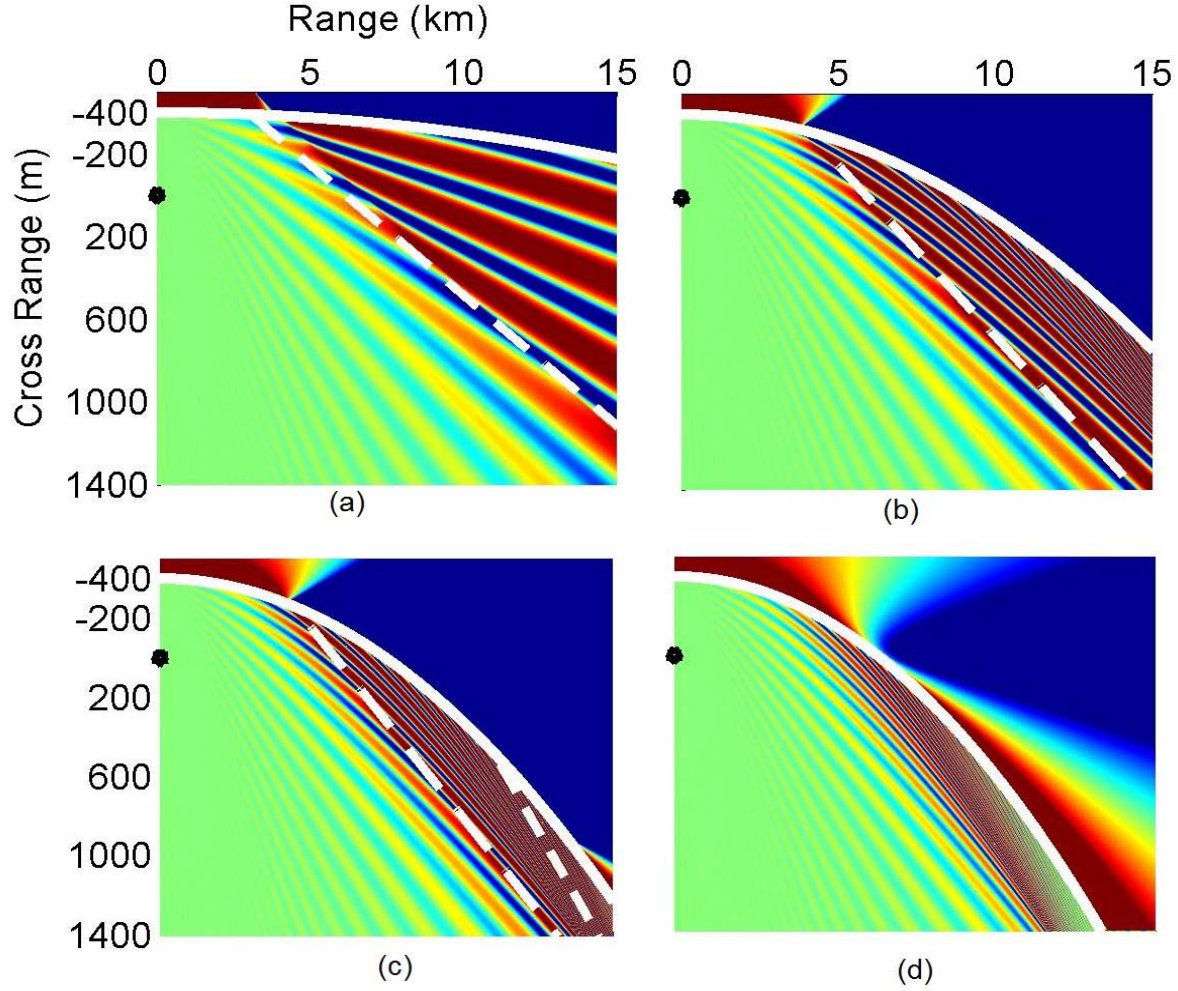


Figure 2. Acoustic modes interacting with nonlinear internal wave fronts at small incident angles may form horizontal Lloyd mirror (HLM) interference patterns that are particularly clear for single modes propagating adiabatically. Color contours of reduced transmission loss are referenced to the direct arrival contribution, so that a 10 dB dynamic range can display the pattern in a horizontal plane with range from 0 to 15 km and cross-range from -400 to 1400 m. A 55 Hz source is located at the origin, and the front is modeled as a sound speed jump of 12 m/s, which if it were straight would lie along cross-range -400 m. Results are shown for a circular wave front, with radius of curvature R and symmetry about the cross-range axis. A front is indicated by solid white lines, and dashed white lines demarcate regions of strong HLM patterns where the front reflection coefficient has magnitude one. Fig. 2(a) with $R = 500$ km shows a strong HLM pattern where total internal reflection occurs, for ranges beyond 3 km and for an increasing spread of cross-range values with range. Fig. 2(b) with $R = 100$ km has a smaller region, beyond 5 km, of strong HLM patterns with narrower beam spacing. Fig. 2(c) with increasing curvature $R = 70$ km continues the trends, with the appearance of the region beyond 10 km where total internal reflection no longer occurs. The region of strong HLM patterns is bounded by two dashed lines and a portion of the front curve, and transmission across the front can be seen for both smaller and larger ranges. Fig. 2(d) with $R = 50$ km shows no region of strong HLM patterns and transmission almost everywhere across the front. Nonlinear internal wave front curvature, along with other parameters, can have important effects on HLM interference patterns.

IMPACT/APPLICATIONS

New or enhanced capabilities for handling physical properties of shallow water sediments, including layering, elasticity, porosity, and anisotropy, are provided for propagation predictions. Range-dependent variability from bathymetry, topography, and sediment layer interfaces in propagation calculations can be treated. Intensity attenuation and coherence statistics that result from environmental fluctuations and experimental variability can be found efficiently. Data analyses and comparisons permit specification, for experimental and application purposes, of the relative significance of key physical mechanisms: linear versus nonlinear frequency dependence of sediment attenuation, sediment heterogeneity versus homogeneity, water column versus bathymetric variability, water column scattering versus refraction, and vertical versus horizontal mode coupling due to internal solitons and bathymetry. Results from modeling and data analyses of experiments, including New Jersey Shelf experiments and the ACT series, are partly aimed toward improving shallow water sonar systems and predictions. Propagation model implementations, analysis tools, and data representation techniques are distributed to university, laboratory, and research and development groups.

RELATED PROJECTS

- Continuing projects with Dr. Michael Collins [3]-[8] also include a monograph on state of the art parabolic wave equation models and applications [23], for which principal research results are nearly complete and chapter drafts are prepared.
- Investigations with Drs. James Lynch and Timothy Duda and their colleagues [9]-[12] are directed toward propagation effects from waveguides and anti-waveguides of variable structure generated by nonlinear internal waves.
- Research with Profs. William Carey and Allan Pierce [13]-[17], [19]-[22] focuses on propagation variability from sediment geoacoustic structure and attenuation, and on modeling seabed properties using their theory for mud structure (future support for PhD student J. O. Fayton from the SMART Scholarship Program).

REFERENCES

- [1] J. M. Collis, W. L. Siegmann, M. Zampoli, and M. D. Collins, "Extension of the rotated elastic parabolic equation to beach and island propagation," *IEEE J. Ocean Eng.* **34**, 617-623 (2009).
- [2] H. J. Simpson, R. J. Soukup, J. M. Collis, M. D. Collins, and W. L. Siegmann, "Experimental testing of the variable rotated elastic parabolic equation." Accepted for publication in *J. Acoust. Soc. Am.*
- [3] A. M. Metzler, W. L. Siegmann, M. D. Collins, and J. M. Collis, "Time-domain solutions for Rayleigh waves and other environments using the single-scattering parabolic equation." See also (A) *J. Acoust. Soc. Am.* **124**, 2585 (2008). In preparation for submission. Supported by OA Graduate Traineeship Award 0972.

- [4] A. M. Metzler, W. L. Siegmann, R. N. Baer, M. D. Collins, and J. M. Collis, “Parabolic equation solutions for anisotropic waves in heterogeneous media.” See also (A) *J. Acoust. Soc. Am.* **125**, 2500 (2009). In preparation for submission. Supported by OA Graduate Traineeship Award 0972.
- [5] M. D. Collins and W. L. Siegmann, “Improving the parabolic equation solution for solutions involving sloping fluid-elastic interfaces.” See also (A) *J. Acoust. Soc. Am.* **127**, 1962 (2010). In preparation for submission.
- [6] A. J. Fredricks, W. L. Siegmann, and M. D. Collins, “Parabolic equation models for anisotropic poro-elastic media.” Submitted for refereed publication.
- [7] A. M. Metzler, W. L. Siegmann, and M. D. Collins, “Improving the parabolic equation solution for problems involving poro-elastic media.” See also (A) *J. Acoust. Soc. Am.* **127**, 1962 (2010). In preparation for submission. Supported by OA Graduate Traineeship Award 0972.
- [8] A. M. Metzler and W. L. Siegmann, “Parabolic equation solutions with increased capabilities for layered poro-elastic media.” See also (A) *J. Acoust. Soc. Am.* **128**, 2479 (2010). In preparation for submission. Supported by OA Graduate Traineeship Award 0972.
- [9] K. G. McMahon, L. K. Reilly-Raska, J. F. Lynch, T. F. Duda, and W. L. Siegmann, “Acoustic propagation through nonlinear internal waves: a horizontal Lloyd mirror model.” See also (A) *J. Acoust. Soc. Am.* **127**, 1963 (2010). Submitted for refereed publication. Supported by OA Graduate Traineeship Award 0638.
- [10] C. C. Boughan Khan, T. F. Duda, J. F. Lynch, A. E. Newhall, and W. L. Siegmann, “Nonlinear internal wave parameter extraction from SAR images.” See also (A) *J. Acoust. Soc. Am.* **124**, 2444 (2008). In preparation for submission.
- [11] L. K. Reilly-Raska, W. L. Siegmann, J. F. Lynch, J. Colosi, and T. F. Duda, “Acoustic mode coupling effects in propagation through nonlinear internal waves.” In preparation for submission.
- [12] K. G. McMahon, J. F. Lynch, Y.-T. Lin, and W. L. Siegmann, “Energy propagation in nonlinear internal wave ducts from radiative transport theory.” See also (A) *J. Acoust. Soc. Am.* **128**, 2335 (2010). In preparation for submission. Supported by OA Graduate Traineeship Award 0638.
- [13] W. J. Saintval, A. D. Pierce, W. M. Carey, and W. L. Siegmann, “A modified Pekeris waveguide for examining sediment attenuation influence on modes.” Submitted for refereed publication.
- [14] W. J. Saintval, W. L. Siegmann, W. M. Carey, and A. D. Pierce, “Parameter sensitivities of modal attenuation coefficients for sandy sediments in the Gulf of Mexico.” See also (A) *J. Acoust. Soc. Am.* **123**, 3594 (2008). Submitted for refereed publication.
- [15] W. J. Saintval, W. L. Siegmann, W. M. Carey, A. D. Pierce, and J. F. Lynch, “Frequency variation of modal attenuation coefficients from sandy-silty shelf environments.” In preparation for submission.

- [16] S. V. Kaczkowski, W. L. Siegmann, W. J. Saintval, A. D. Pierce, and W. M. Carey, “Parametric variations of modal attenuation coefficients obtained from modal approximations.” In preparation for submission.
- [17] W. J. Saintval, W. L. Siegmann, W. M. Carey, A. D. Pierce, and J. F. Lynch, “Estimation of effective attenuation coefficients from the New Jersey Shelf environment.” In preparation for submission.
- [18] M. Jaye, J. S. Robertson, W. L. Siegmann, and M. Badiey, “Broadband propagation over randomly varying, range-dependent elastic sediments.” Submitted for refereed publication.
- [19] S. V. Kaczkowski, W. M. Carey, A. D. Pierce, and W. L. Siegmann, “Relationships between intrinsic sediment attenuation, modal attenuation, and transmission loss in experimental environments over sandy-silty sediments.” See also (A) *J. Acoust. Soc. Am.* **126**, 2167 (2009). In preparation for submission.
- [20] S. V. Kaczkowski, W. M. Carey, A. D. Pierce, and W. L. Siegmann, “Averaged transmission loss expressions in shallow water waveguides with sandy-silty sediments.” See also (A) *J. Acoust. Soc. Am.* **128**, 2480 (2010). In preparation for submission.
- [21] J. O. Fayton, A. D. Pierce, W. M. Carey, and W. L. Siegmann, “The card-house structure of mud: energy between particles and its effect on bubble formation.” See also (A) *J. Acoust. Soc. Am.* **127**, 1938 (2010). In preparation for submission.
- [22] J. O. Fayton, A. D. Pierce, W. M. Carey, and W. L. Siegmann, “The card-house structure of mud: determination of shear wave speed.” See also (A) *J. Acoust. Soc. Am.* **128**, 2357 (2010). In preparation for submission.
- [23] M. D. Collins and W. L. Siegmann, *Parabolic Wave Equations with Applications*. In preparation for Springer-Verlag publishers.

PUBLICATIONS

- Published [refereed]: [1]
- Accepted [refereed]: [2]
- Submitted [refereed]: [6], [9], [13], [14], [18]